Optimization of Hydrogen Production from a Proton-Conducting Solid Oxide Electrolysis Cell

CHAWANUT TANGKUSONJIT

A Report Submitted in Partial Fulfillment of the Requirements
for the Degree of Bachelor of Engineering (Petrochemical Engineering)
Department of Chemical Engineering, Faculty of Engineering,
King Mongkut's Institute of Technology Ladkrabang
Academic Year 2017

การหาสภาวะที่เหมาะสมสำหรับการผลิตแก๊สไฮโดรเจนจากเซลล์อิเล็กโทรไลซิสชนิดออกไซด์แข็งแบบนำโปรตอน

เชาวณัฐ ตั้งกุศลจิต

ปริญญานิพนธ์นี้เป็นส่วนหนึ่งของการศึกษาตามหลักสูตร
วิศวกรรมศาสตรบัณฑิต สาขาวิชาวิศวกรรมปิโตรเคมี
ภาควิชาวิศวกรรมเคมี คณะวิศวกรรมศาสตร์
สถาบันเทคโนโลยีพระจอมเกล้าเจ้าคุณทหารลาดกระบัง
ปีการศึกษา 2560

Title	Optimization of Hydrogen Production from a Proton-Conducting Solid Oxide Electrolysis Cell
By	Mr.Chawanut Tangkusonjit
Field of Study	Petrochemical Engineering
Advisor	Assist. Prof. Dr.Yaneeporn Patcharavorachot

Accepted by the Faculty of Engineering, King Mongkut's Institute of Technology Ladkrabang in Partial Fulfillment of the Requirements for the Degree of Bachelor of Engineering (Petrochemical Engineering).

Thesis Committee

_____ Chairman
(Assist. Prof. Dr.Yaneeporn Patcharavorachot)

_____ Committee
Assoc. Prof. Dr. Duangkamol Na-Ranong)

_____ Committee
(Assist. Prof. Dr. Nuttapol Lerkkasemsan)

Title	Optimization of Hydrogen Production from a Proton-Conducting Solid Oxide Electrolysis Cell
By	Mr. Chawanut Tangkusonjit
Advisor	Assist. Prof. Dr. Yaneeporn Patcharavorachot
Field of Study	Petrochemical Engineering
Affiliation	

Abstract

This project focuses on hydrogen production from a proton-conducting solid oxide electrolysis cell (H-SOEC). This method has been received much attention since H-SOEC can operate at low temperature condition. Moreover, It can consume electricity from renewable energy so it is green technology to produce hydrogen. The AspenPlusTM simulator is used as tool for a performance analysis of H-SOEC. The simulation result obtained from an electrochemical model is compared with the experimental data extracted from the literature to ensure that a proposed model can predict the behavior of H-SOEC. It is found that the model prediction is agree with the experimental result. Then, the effect of key operating condition, e.g., temperature, pressure, steam flow rate and current density, on cell voltage and hydrogen production is investigated. In addition, the optimization is performed to idenify the optimal operating condition of H-SOEC, response surface method is used to find the optimization condition of H-SOEC. The result indicated that the values of temperature, pressure, steam flow rate and current density affect to cell voltage and hydrogen content. In order to provide the minimized cell voltage, H-SOEC should be operated at temperature of 713°C, pressure of 1 bar, steam flow rate of 372 kmol/h and current density of 1000 A/m^2. Under this operating condition, it can provide hydrogen as 333 kmol/h.

Keywords: Optimization, Simulation, Proton-conducting solid oxide electrolysis cell, Hydrogen production, Solid oxide electrolysis cell, Proton-conducting electrolyte

เรื่อง	การหาสภาวะที่เหมาะสมสำหรับการผลิตแก๊สไฮโดรเจนจากเซลล์อิเล็กโทรไล--ซิสชนิดออกไซด์แข็งแบบนำโปรตอน
โดย	นายเชาวณัฐ ตั้งกุศลจิต
อาจารย์ที่ปรึกษา	ผศ.ดร.ญาณีพร พัชรวรโชติ
สาขาวิชา	ปิโตรเคมี
สังกัด	

บทคัดย่อ

โครงงานนี้มีจุดประสงค์มุ่งเน้นเพื่อทำการศึกษาเกี่ยวกับการผลิตแก๊สไฮโดรเจนจากเซลล์อิเล็กโทรไลซิสชนิดออกไซด์แข็งแบบนำโปรตอน (H-SOEC) เนื่องจากเซลล์อิเล็กโทรไลซิสชนิดออกไซด์แข็งแบบนำโปรตอนสามารถทำงานได้ที่อุณหภูมิต่ำ ยิ่งไปกว่านั้นสามารถใช้พลังงานไฟฟ้าจากแหล่งพลังงานทางเลือกซึ่งเป็นวิธีการผลิตที่เป็นมิตรต่อสิ่งแวดล้อม โดยจะใช้โปรแกรม AspenPlus™ เป็นเครื่องมือในการจำลองการทำงานของเซลล์อิเล็กโทรไลซิสชนิดออกไซด์แข็งแบบนำโปรตอน ซึ่งผลของการจำลองจากแบบจำลองไฟฟ้าจะถูกนำไปเปรียบเทียบกับผลการทดลองจริงจากทบทวนวรรณกรรมเพื่อที่จะทำการทำนายว่าการจำลองเป็นไปตามพฤติกรรมของเซลล์อิเล็กโทรไลซิสชนิดออกไซด์แข็งแบบนำโปรตอน และพบว่าผลของการจำลองตรงตามการทดลองจริง โดยจะทำการทดลองเกี่ยวกับปัจจัยที่อาจจะส่งผลต่อศักย์ไฟฟ้าของเซลล์และปริมาณแก๊สไฮโดรเจน เช่น อุณหภูมิ ความดัน อัตตาตราการไหลของไอน้ำและกระแสไฟฟ้า ยิ่งไปกว่านั้นโครงงานนี้ยังทำการเพิ่มประสิทธิภาพโดยการหาสภาวะที่เหมาะสมโดยใช้วิธีพื้นผิวตอบสนองในการวิเคราะห์และจากผลการทดลองจะแสดงให้เห็นว่า อุณหภูมิ ความดัน อัตตราการไหลของไอน้ำและกระแสไฟฟ้าส่งผลต่อศักย์ไฟฟ้าของเซลล์และปริมาณแก๊สไฮโดรเจน จึงพบว่าการที่จะได้ค่าศักย์ไฟฟ้าของเซลล์ต่ำสุดจะต้องใช้อุณหภูมิที่ 713 องศาเซลเซียส ความดัน 1 บาร์ อัตตราการไหลของน้ำ 373 กิโลโมลต่อชั่วโมง ต่อกระแสไฟฟ้า 1000 แอมแปร์ต่อตารางเมตร ซึ่งจะทำให้ได้ปริมาณแก๊สไฮโดรเจน 333 โมลต่อชั่วโมง

คำสำคัญ: สภาวะที่เหมาะสม, การจำลอง, เซลล์อิเล็กโทรไลซิสชนิดออกไซด์แข็งแบบนำโปรตอน, เซลล์อิเล็กโทรไลซิสชนิดออกไซด์แข็ง, การผลิตไฮโดนเจน, อิเล็กโทรไลแบบนำโปรตอน

Acknowledgements

For this project, I am thankful my advisor, Assist.Prof.Dr.Yaneeporn Patcharavorachot for introduction to interesting project, helping, advising and discussion throughout the work until completed. Moreover, I would like to thank my family and professor that not mentioned but educate, encourage and support me.

Finally, if the project has some mistake, I apologize.

Mr.Chawanut Tangkusonjit

Table of Contents

Table of Contents (cont)

Page

List of Figure

Page

List of Table

Page

Symbols

Symbols	Meaning	Unit
V	Cell potential	V
E	Reversible potential	V
η_{ohm}	Ohmic overpotential	V
$\eta_{conc,anode}$	Concentration overpotentials at anode	V
$\eta_{conc,cathode}$	Concentration overpotentials at cathode	V
$\eta_{act,anode}$	Activation overpotentials at anode	V
$\eta_{act,cathode}$	Activation overpotentials at cathode	V
E^0	Standard potential	V
R	Gas constant	8.314 J/K·mol
T	Operating temperature	K
F	Faraday constant	9.6485×10^4 C/mol
P_i	Partial pressure of species i	bar
j	Current density	Am/m^2
R_{ohm}	Ohm resistant	$\Omega \cdot m^2$
$\tau_{electrode}$	Cell thickness of electrode	100×10^{-6} m
$\tau_{electrolyte}$	Cell thickness of electrolyte	100×10^{-6} m
$\rho_{electrolyte}$	Conductivity of electrolyte	$7.66 \times 10^6/(T \cdot \exp(-8.74 \times 10^3/T))$ $\Omega^{-1}m^{-1}$
P_i^{TPB}	Partial pressure of species i at Triple Phase Boundary (TPB)	bar
D_i^{eff}	Effective diffusion coefficient of the species i	m^2s^{-1}
P	Operating pressure	bar
ϕ	Electrode tortuosity	$(1.5-0.5\varepsilon)^{1/2}$
ξ	Electrode porosity	0.3
$D_{i,j}$	Binary diffusion coefficients of species i and j	m^2s^{-1}
$D_{i,K}$	Knudsen diffusion coefficients of species i	m^2s^{-1}
$\sigma_{i,j}$	Characteristic length of species i	Å
Ω_D	Diffusion collision integral	-
M_i	Molecular weight of species i	$g \cdot mol^{-1}$
k_B	Boltzmann's constant	1.3804×10^{23} $J \cdot K^{-1}$
$\bar{r}$	Mean electrode pore radius	m
$j_{0,cathode}$	Exchange current densities at the cathode	Am/m^2
$j_{0,anode}$	Exchange current densities at the anode	Am/m^2
k_{anode}	Pre-potential factors of anode	2.802×10^5 $\Omega^{-1} \cdot m^{-2}$
$k_{cathode}$	Pre-potential factors of cathode	8.569×10^5 $\Omega^{-1} \cdot m^{-2}$
E_a	Activation energy levels at the anode	53.123 $kJ \cdot mol^{-1}$
E_c	Activation energy levels at the cathode	56.739 $kJ \cdot mol^{-1}$
$\dot{n}_i$	Molar flow rate of species i	kmol/h

CHAPTER I
INTRODUCTION

1.1 Background

In the present, hydrogen is used in several objectives such as hydrocracking process, ammonia production, methanol production and fuel. Hydrogen becomes an alternative fuel in engine; it tends to be used instead of gasoline or diesel since it can reduce the emission of carbon dioxide and sulfur to the atmosphere which are cause of climate change. Global warming is changing average temperature of the earth. The emission of carbon dioxide and other greenhouse gases causes global surface temperature to rise average 1.7° since 1880 to the present [1]. Moreover, the concentration of carbon dioxide in the world tends to increase from 378 parts per million in January 16, 2005 to 406 parts per million in September 16, 2017 [1]. Therefore, the hydrogen production without carbon dioxide emission has been considered in this project.

Annually, the demand of hydrogen has been increasing 3.5 percent until 2018 more than 300 billion cubic meters [2]. In general, hydrogen can be produced from many technologies such as steam reforming, thermolysis and electrolysis. In order to produce hydrogen without carbon dioxide emission, this project focuses on hydrogen production through the water electrolysis. The water electrolysis uses the electricity to separate water and then, hydrogen and oxygen is generated. If the electricity produces from renewable energy such as solar, wind, wave and nuclear energy that are clean technology, hydrogen production through the water electrolysis becomes the cleanest method.

Among many kinds of electrolysis, the solid oxide electrolysis cell (SOEC) has received much interest since it requires low energy consumption and provides high efficiency of conversion [3]. In general, there are two types of electrolyte possible to use in SOEC, i.e., oxygen conducting (O-SOEC) and proton conducting (H-SOEC). The H-SOEC is better than O-SOEC since it can produce pure hydrogen at the cathode side and require low temperature operation about 500 to 800 °C [4].

Because the investigation on H-SOEC has been limited, some parameters are unknown. Then, the effect of operating condition (temperature, pressure and feed ratio) on hydrogen production is examined.

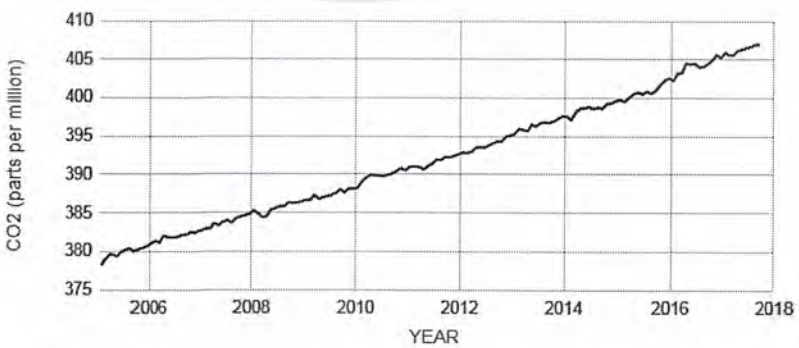

Fig. 1.1 Concentration change of carbon dioxide in the world [1]

Finally, the optimization is performed to determine the optimal conditions that maximizing hydrogen content and minimizing cell potential.

1.2 Objectives

Study the important parameters on hydrogen production through H-SOEC and determine the optimal conditions that providing the maximum hydrogen content and the minimum hydrogen.

1.3 Scope of Work

1.3.1 Design the model of H-SOEC for hydrogen production in Aspen Plus simulator
1.3.2 Validate the simulation results with the experimental data from the literature
1.3.3 Study the effect of important operating conditions, e.g., temperature, pressure, inlet steam flow rate and current density on hydrogen production
1.3.4 Perform optimization of H-SOEC operation to maximize hydrogen content and minimize cell potential

1.4 Expected Outputs

1.4.1 The developed electrochemical model can be further used by other researchers.
1.4.2 The simulation results can be used a guideline in the real operation.

CHAPTER II
THEORY LITERATURE REVIEW

This chapter presents theorem of proton-conducting solid oxide electrolysis cell (H-SOEC) that uses for hydrogen production. The basic component, principle, electrochemical model and materials used of H-SOEC are also included in this chapter. Moreover, the literature review is summarized.

2.1 Proton-conducting solid oxide electrolysis cell (H-SOEC)

The proton-conducting solid oxide electrolysis cell or H-SOEC has main three parts that include cathode, electrolyte and anode. Fig. 2.1 presents the components and operation of H-SOEC. In the operation, steam is fed at the anode side where it is oxidized to oxygen, protons and electrons (Eq. (2.1)). The protons will transfer from the anode side through the electrolyte to the cathode side. At the cathode side, the protons react with electrons to produce hydrogen (Eq. (2.2)). It can be observed that pure hydrogen can be produced at the cathode side. Therefore, the purification unit can be eliminated in H-SOEC operation and this is main advantage of H-SOEC over O-SOEC. The chemical reactions occurred in H-SOEC operation are shown below:

Anode: $H_2O \rightarrow \frac{1}{2}O_2 + 2H^+ + 2e^-$ (2.1)

Cathode: $2H^+ + 2e^- \rightarrow H_2$ (2.2)

Overall: $H_2O \rightarrow \frac{1}{2}O_2 + H_2$ (2.3)

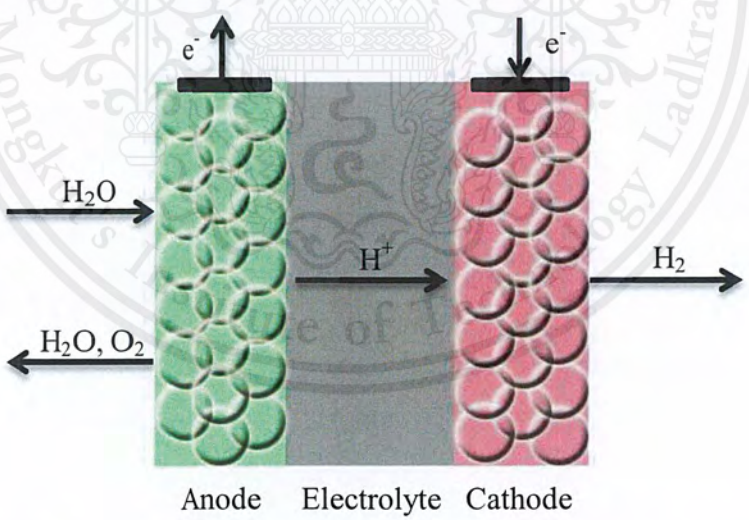

Fig. 2.1 The basic component and operation of the H-SOEC

2.2 Electrochemical model

Electrochemical model can predict the performance of H-SOFC which presents the relationship between current density (j) and cell potential (V). Not only the operating conditions (e.g., temperature, pressure and fed component) but also structural parameters (e.g., thickness of each component) have a significant effect on the H-SOEC performance. The real cell potential is the summation of reversible potential (E) and voltage losses which can be expressed as:

$$V = E + \eta_{ohm} + \eta_{conc,anode} + \eta_{conc,cathode} + \eta_{act,anode} + \eta_{act,cathode} \quad (2.4)$$

The reversible potential (E) is minimum potential of electrolysis cell consumed which can be calculated from the Nernst equation as follows:

$$E = E^0 + \frac{RT}{2F} ln(\frac{P_{H_2} P_{O_2}^{\frac{1}{2}}}{P_{H_2O}}) \quad (2.5)$$

where E^0 is standard potential; R is the gas constant; T is the operating temperature; F is Faraday's constant; P_i is the partial pressure of each species. The standard potential can be given as the below equation [5].

$$E^0 = 1.253 - 0.00024516T \quad (2.6)$$

However, the potential of the cell potential (V) would be more than the reversible potential (η) because there are potential losses which include ohmic overpotential (η_{ohm}), concentration overpotentials at anode ($\eta_{conc,anode}$) and cathode ($\eta_{conc,cathode}$) and activation overpotentials at anode ($\eta_{act,anode}$) and cathode ($\eta_{act,cathode}$).

2.2.1. Ohmic overpotential

In matter of facts, the electrical conductivity of electrode at cathode and anode is higher than the electrolyte ($\rho_{electrode} \gg \rho_{electrolyte}$). Thus, the electrode value can be neglected. The ohmic overpotential is calculated Ohm's law as Eq. (2.7)-(2.8):

$$\eta_{ohm} = j \times R_{ohm} \quad (2.7)$$

$$R_{ohm} = \frac{\tau_{electrode}}{\rho_{electrode}} + \frac{\tau_{electrolyte}}{\rho_{electrolyte}} \approx \frac{\tau_{electrolyte}}{\rho_{electrolyte}} \quad (2.8)$$

where $\tau_{electrode}$ and $\tau_{electrolyte}$ are the cell thickness of electrode and electrolyte, respectively; $\rho_{electrode}$ and $\rho_{electrolyte}$ are the conductivity of electrode and electrolyte, respectively.

2.2.2. Concentration overpotentials

The concentration overpotentials are the resistance to mass transport of gas species at the electrode-electrolyte interface (Triple Phase Boundary, TPB). The concentration overpotential at the anode and cathode can be computed by Eqs. (2.9) and (2.10), respectively.

$$\eta_{conc,anode} = \frac{RT}{2F}\ln[\left(\frac{P_{H_2O}}{P_{H_2O}^{TPB}}\right)\left(\frac{P_{O_2}^{TPB}}{P_{O_2}}\right)^{\frac{1}{2}}] \tag{2.9}$$

$$\eta_{conc,cathode} = \frac{RT}{2F}\,ln\left(\frac{P_{H_2}^{TPB}}{P_{H_2}}\right) \tag{2.10}$$

The partial pressures of H_2O, O_2 and H_2 at TPB derived from Fick's law are shown in the following equations.

$$P_{H_2O}^{TPB} = P_{H_2O} - \frac{RT\tau_{anode}}{2FD_{H_2O}^{eff}}j \tag{2.11}$$

$$P_{O_2}^{TPB} = P_{O_2} - \frac{RT\tau_{anode}}{4FD_{O_2}^{eff}}j \tag{2.12}$$

$$P_{H_2}^{TPB} = P - \left(P - P_{H_2}\right)exp(-\frac{RT\tau_{cathode}}{2FD_{H_2}^{eff}}j) \tag{2.13}$$

where D_i^{eff} is the effective diffusion coefficient of the species i; P is the operating pressure. The effective diffusion coefficient can be explained in the Bosanquet equation as Eq. (2.14);

$$\frac{1}{D_i^{eff}} = \frac{\phi}{\xi}(\frac{1}{D_{i,j}} + \frac{1}{D_{i,K}}) \tag{2.14}$$

where ϕ is the electrode tortuosity; ξ is the electrode porosity; and $D_{i,j}$ *and* $D_{i,K}$ are the binary and Knudsen diffusion coefficients, respectively. The electrode tortuosity determined from [6] in Eqs. (2.15) and (2.16) shows the binary diffusion coefficient based on the ideal-gas law from [7];

$$\phi = (\frac{3-\xi}{2})^{\frac{1}{2}} \tag{2.15}$$

$$D_{i,j} = \frac{0.00266T^{3/2}}{PM_{i,j}^{1/2}\sigma_{i,j}^2\Omega_D} \tag{2.16}$$

where $\sigma_{i,j}$ is the mean characteristic length of the species i and j; Ω_D is the diffusion collision integral; M_i is the molecular weight of each species. The all variables can be determined in Eqs. (2.17)-(2.20);

$$M_{i,j} = 2(\frac{1}{M_i} + \frac{1}{M_j})^{-1} \quad (2.17)$$

$$\sigma_{i,j} = \frac{\sigma_i + \sigma_j}{2} \quad (2.18)$$

Table 2.1 Parameters for effective diffusion coefficient calculation [7].

	H_2O	H_2	O_2
σ_i(Å)	2.641	2.827	3.467
ε_i/k_B(K)	809.1	59.7	106.7

$$\Omega_D = \frac{1.06036}{\Gamma^{0.15610}} + \frac{0.19300}{\exp(0.47635\Gamma)} + \frac{1.03587}{\exp(1.52996\Gamma)} + \frac{1.76474}{\exp(3.89411\Gamma)} \quad (2.19)$$

$$\Gamma = \frac{k_B T}{(\varepsilon_i \varepsilon_j)^{1/2}} \quad (2.20)$$

where σ_i is the characteristic length of the species i; k_B is the Boltzmann's constant. The value of σ_i and ε_i/k_B are found in Table 2.1.

From the Eq. (14), the Knudsen diffusion coefficient can be derived from the kinetic theory of gases [8] and expressed as Eq. (2.21)

$$D_{i,K} = \frac{2}{3}(\frac{8RT}{\pi M_i})^{1/2}\bar{r} \quad (2.21)$$

where $\bar{r}$ is the mean pore radius.

2.2.3. Activation overpotentials

The activation ovepotentials are loss due to the kinetic reactions at the electrodes. The Butler-Volmer equation is used to calculate these losses as Eqs. (2.22)-(2.23);

$$\eta_{act,anode} = \frac{RT}{F} sinh^{-1}(\frac{j}{2j_{0,anode}}) \quad (2.22)$$

$$\eta_{act,anode} = \frac{RT}{F} sinh^{-1}(\frac{j}{2j_{0,cathode}}) \quad (2.23)$$

where $j_{0,cathode}$ and $j_{0,anode}$ are the exchange current densities at the cathode and anode. In general, the exchange current density is defined in several forms. It can be constant value or depends on operating conditions. Since the operating conditions are affected to the performance of H-SOEC, the constant exchange current density may result in the different performance between the calculation and real operation. Thus,

this thesis aims to develop the exchange current density in the format of Arrhenius equation as follows:

$$j_{0,anode} = \frac{RT}{2F} k_{anode} \exp\left(-\frac{E_{a,anode}}{RT}\right) \quad (2.24)$$

$$j_{0,cathode} = \frac{RT}{2F} k_{cathode} \exp\left(-\frac{E_{a,cathode}}{RT}\right) \quad (2.25)$$

where γ_a and γ_c are pre-potential factors of anode and cathode, respectively;
E_a and E_c are the activation energy levels at the anode and cathode, respectively;

Table 2.2 Pre-potential factors and activation energy levels

k_{anode}	$2.802\times10^5\ \Omega^{-1}\cdot m^{-2}$	E_a	$53.123\ kJ\cdot mol^{-1}$
$k_{cathode}$	$8.569\times10^5\ \Omega^{-1}\cdot m^{-2}$	E_c	$56.739\ kJ\cdot mol^{-1}$

The materials have different an advantage and the exchange current density (j_0). Therefore, this project has to use the results of voltage (V) and current density (j) from real experiment to plot graph compare with the results from simulation program for confirmation which the results is followed theorem.

2.3 Design of Experiment (DOE)

The design of experiment (DOE) is a potential method for engineering. Generally, DOE is used to calculate number of the experiment. The important variables affected on the experiment can be also justified. In addition, DOE can help to reduce time and cost in improving the process.

2.3.1 Response Surface Method (RSM)

The response surface method (RSM) is one of methods in DOE for determination of optimum operating conditions of the process. RSM represents an equation of independent variable (y1) or surface area between independent and dependent variables.

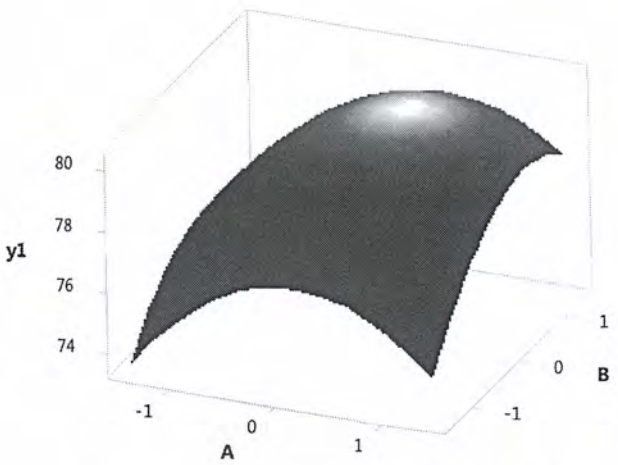

Fig. 2.2 Presents the example of surface plot by RSM

Normally, first-order model is used in low-order polynomial as a linear function. It can be expressed as Eq. (2.26);

$$y = \beta_0 + \beta_1 x_1 + \beta_2 x_2 + \cdots + \beta_k x_k + \epsilon \tag{2.26}$$

where ϵ is noise or error.

Second-order model is used in high-order polynomial as a curvature in the system. It can be expressed as Eq. (2.27);

$$y = \beta_0 + \sum_{i=1}^{k} \beta_i x_i + \sum_{i=1}^{k} \beta_{ii} x_i^2 + \sum\sum_{i<j} \beta_{ij} x_i x_j + \epsilon \tag{2.27}$$

2.3.2 Box-Behnken

Box and Behnken (1960) had been proposing 3 level designs for suitable response surfaces. These designs are combination between 2^k factorials and incomplete block designs. The designed results are greatly efficient for the used number of the experiment.

The Box–Behnken design does not contain any points at the vertices of the cubic box which created by the upper and lower limits for each variable where, the face-centered central composite contain every points at the corner and center of the cubic surface so the number of the experiment of the Box-Behnken is used less than the face-centered central composite. This reason can be advantage when the points on the corners of the cube represent factor-level combinations which are impossible for testing because physical process constraints. [9]

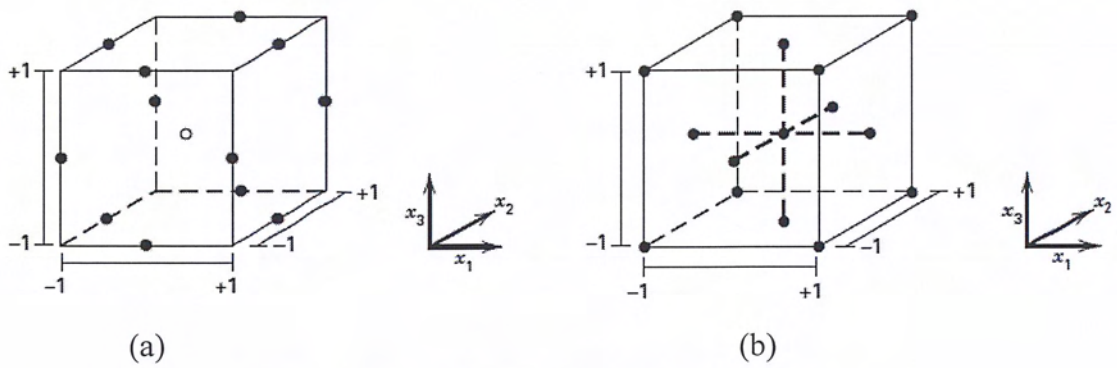

Fig. 2.3 Three factors design for (a) Box-Behnken and (b) face-centered central composite [9]

2.4 Literature review

L. Bi et al. [4] studied and analyzed reversible solid fuel cells (R-SOFCs) in which using different electrode and electrolyte were considered. They used Ni-based electrode and $BaZrO_3$ and $BaCeO_3$ electrolyte in this experiment. The results of the J-V characteristics in R-SOFC mode and SOFC mode were compared. The results indicated that the $BaZrO_3$ proton conductivity better than $BaCeO_3$. Moreover, The $BaZrO_3$ is easily sinterable and easy to fabricate in electrolyte film. In the other hand, The Ni-based is suitable to be used as electrode due to low cost, high conductivity and good chemical compatibility with proton-conducting electrolyte materials. Finally, they concluded that the $BaZrO_3$ is absolutely interested in the future.

L. Namwong et al. [10] studied modeling and optimization of the H-SOEC for hydrogen and syngas production. The simulation was done in Aspen Plus software to calculate cell potential and flow rate of hydrogen and carbon dioxide. Respones surface methode (RSM) is used to analyze the results as statistic value and then, the response equation can be obtained. Their results revealed that the steam flow rate of 7.71 kmol/h at 650°C with 1 atm were the best condition that provides the maximimun carbon dioxide as 1.94 kmol/h and the minimum cell potential as 4.73 V.

M. Ni et al. [11] studied the electrochemical model and mechanisms of the H-SOEC about current density-voltage characteristics with several overpotentials such as activation, ohmic and concentration and the others variable relation for hydrogen production. The results showed that the H-SOEC was better performance when it was operated at high temperature and steam molar flow rate.

N. Visitdumrongkul et al. [12] studied modeling and simulation of SOEC by using Aspen Plus software. From the simulation results, it was found that the cell voltage and overall overpotential decrease with an increase in temperature. This is because higer temperature operation leads to decresing ohmic and activation ovepotentials.

P.A. Satuart et al. [13] studied behavier of H-SOEC that made from $BaCe_{0.9}Y_{0.1}O_{3-\delta}$ (BCY10) at 200-600°C. The results of BCY10 were compared and analysed with $BaZr_{0.9}Y_{0.1}O_{3-\delta}$ (BZY10) about conductivity and potential loss. The BZY10 has lower conductivity than BCY10. In the other hand, the large potential loss were found at lower temperature.

CHAPTER III
RESEARCH METHODOLOGY

In this thesis, hydrogen production from the proton-conducting solid oxide electrolysis cell (H-SOEC) is investigated by using Aspen Plus program version 9. The effect of operating condition on hydrogen production and H-SOEC performance is examined. Then, the optimization is performed by using Minitab to find the optimal conditions that provide the maximum hydrogen content and the minimum cell potential. Section 3.1 presents the model of H-SOEC designed in Aspen Plus simulator. Section 3.2 describes about the design of experiment. Finally, the simulation approach is explained in Section 3.3.

3.1 Flow sheet of hydrogen production through H-SOEC

The following assumptions are made to develop and simulate hydrogen production through H-SOEC.

1) Steady state operation
2) Uniform temperature at the anode, electrolyte and cathode
3) Ideal gas behavior
4) 100% Efficiency of each unit operation

Fig. 3.1 presents the flow sheet of H-SOEC designed in Aspen Plus. Water at 25°C and 1 atm is fed into MIX1 and then, sent to heater (HEAT1) followed by pump (PUMP1) to increase temperature and pressure as the desired value. In the simulation, when steam is supplied to the anode (ANODE), it is assumed that the water separation is carried out at the anode side and the product is composed of hydrogen and oxygen. The unreacted steam is further separated from the product through the electrolyte (ELECTROL), as represented by separator model. Then, hydrogen is removed at the cathode (CATHODE). The details of each component are described as below:

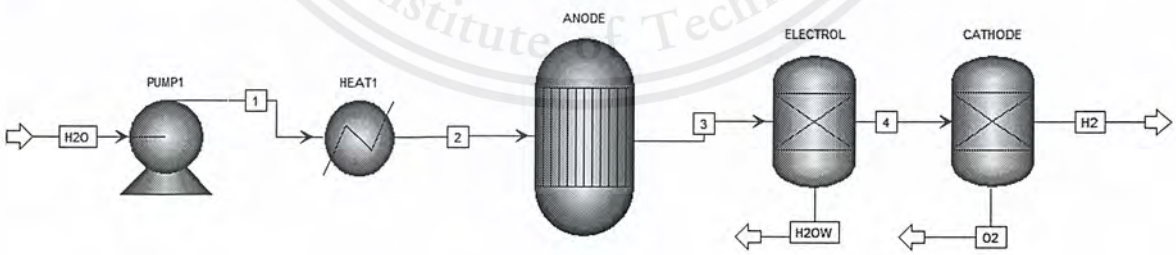

Fig. 3.1 The flowsheet of H-SOEC designed in Aspen Plus.

3.1.1 Anode

The *Rstoic* model is used to replace the anode side in simulation because the reaction is non-spontaneous reaction. The chemical reaction as Eq. (2.3) is assumed to be occurred in the anode side. The conversion of reaction (X) which represents the steam utilization can be expressed by [8]

$$X = \frac{jAN_{cell}}{2F\dot{n}_{H_2O,Feed}} \tag{3.1}$$

where X is the conversion, j is the current density, A is the active area of cell, N_{cell} is the number of cells, F is Faraday's constant and $\dot{n}_{H_2O,Feed}$ is molar flow rate of H_2O fed into the anode, respectively;

3.1.2 Electrolyte

The *Sep* model is represented the electrolyte. It is used for separating the unreacted steam from the product, consisting of oxygen and hydrogen.

3.1.3 Cathode

To separate hydrogen from oxygen, the *Sep* model is introduced to use instead of the cathode side.

The flowsheet of H-SOEC designed in Aspen Plus simulator is used to examine the effect of operating conditions, such as, temperature, pressure, current density and inlet steam flow rate on cell potential and hydrogen content.

3.2 Design of experiment (DOE)

The DOE is used to find the number of the experiment which depended on selected method. In this work, the response surface method (RSM) is selected to determine the optimal operating condition for hydrogen production through H-SOEC. In general, there are many types of RSM as shown in Fig. 3.5. In this work, the Box-Behnken design with three independent variables is used. As seen in Fig. 3.5, it is found that the experiment should be performed as 15 runs. In the experiment, it has to assume maximum, middle and minimum value of each variable as a 1, 0 and -1. For example, 1, 0 and -1 represent 500°C, 400°C and 300°C that are maximum, middle and minimum value of temperature, respectively. Then, the experiment is design as shown in Fig. 3.6. The cell potential and hydrogen flow rate are used as response. It is noted that this work performs the simulation to determine the performance of H-SOEC and thus, the number of experiment is number of simulation. When the simulation is done followed by Fig. 3.6, the statistic and mathematic values can be provided and used in the analysis.

Available Response Surface Designs

Design		Continuous Factors								
		2	3	4	5	6	7	8	9	10
Central composite full	unblocked	13	20	31	52	90	152			
	blocked	14	20	30	54	90	160			
Central composite half	unblocked				32	53	88	154		
	blocked				33	54	90	160		
Central composite quarter	unblocked							90	156	
	blocked							90	160	
Central composite eighth	unblocked									158
	blocked									160
Box-Behnken	unblocked		15	27	46	54	62		130	170
	blocked			27	46	54	62		130	170

Fig. 3.2 Response surface designs

	C1	C2	C3	C4	C5	C6
	RunOrder	A	B	C	Cell Potential	Molar flow rate of H2
1	1	-1	-1	0		
2	2	1	-1	0		
3	3	-1	1	0		
4	4	1	1	0		
5	5	-1	0	-1		
6	6	1	0	-1		
7	7	-1	0	1		
8	8	1	0	1		
9	9	0	-1	-1		
10	10	0	1	-1		
11	11	0	-1	1		
12	12	0	1	1		
13	13	0	0	0		
14	14	0	0	0		
15	15	0	0	0		

Fig. 3.3 Design of the experiment by Box-Behnken method

3.3 Simulation approach

This section explains the procedure of simulation as step by step. The study is divided into two main parts: (1) the investigation of cell potential and hydrogen production with a wider range of operating conditions and (2) the optimization of hydrogen production.

3.3.1 Investigation of cell potential and hydrogen production

As given operating conditions, the composition of each product can be determined. Then, the cell potential is calculated in the calculator block where the electrochemical model presented in Section 2.2 is written. Effect of three important parameters on the cell potential and hydrogen production is examined. Four parameters for investigation that are listed as below:

1). Temperature (T)

2). Pressure (P)
3). Molar flow rate of water ($\dot{n}_{H_2O}$)
4). Current density (i)

3.3.2 Optimization of hydrogen production

To perform the optimization through RSM, the simulation is firstly run as the experimental design. All results are analyzed through Minitab software. From statistic values, the RSM model which presents the relationship between dependent and independent variables can be provided. Finally, the statistic values and RSM equation are used to find the optimal operating condition that maximizing hydrogen production. Four parameters and their operational range are listed as below:

1). Temperature (T): 450-800°C
2). Pressure (P): 1-10 atm
3). Molar flow rate of water ($\dot{n}_{H_2O}$): 100-400 kmol/h
4). Current density (i): 200-1000 Am/m^2

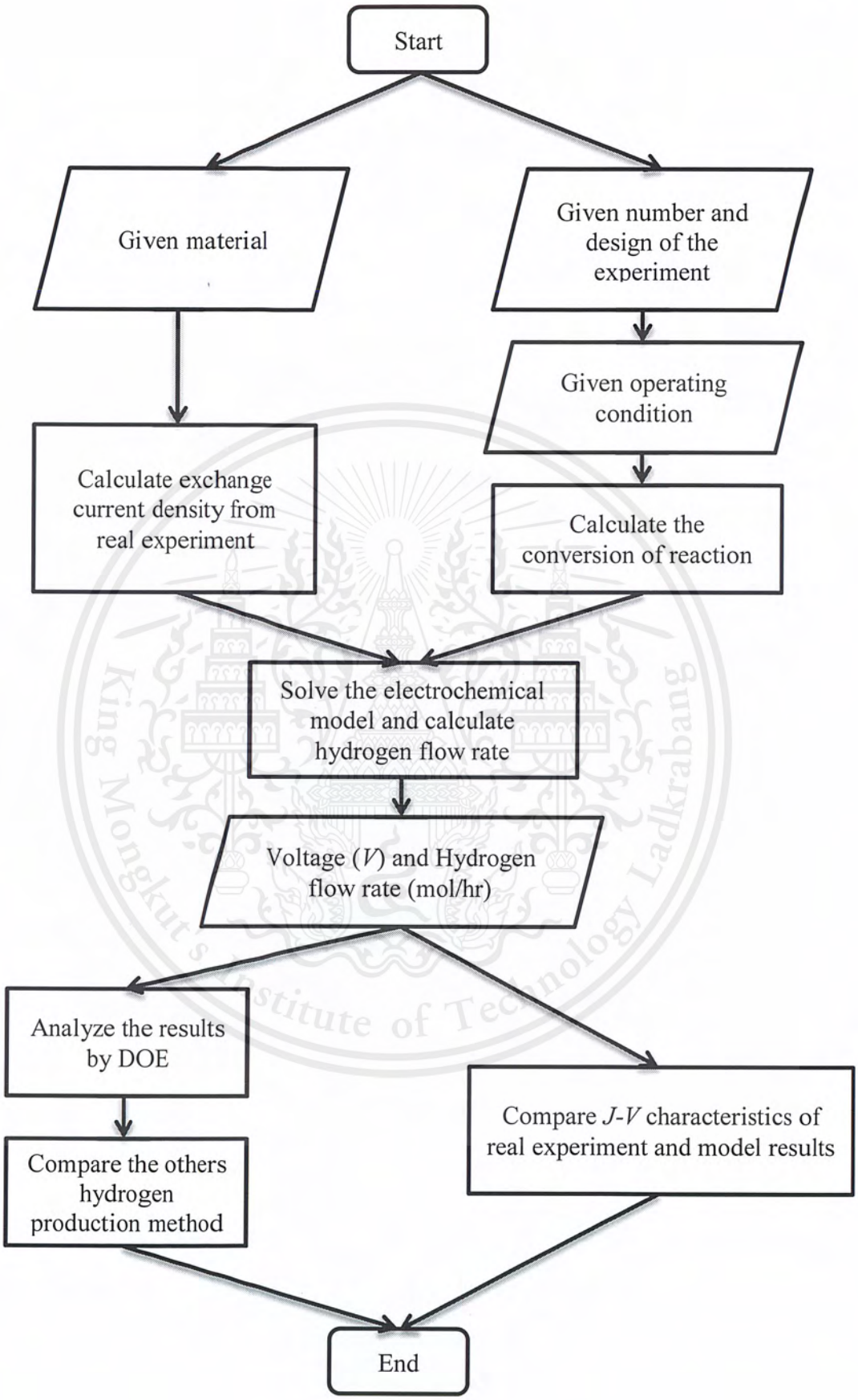

CHAPTER IV
RESULTS AND DISCUSSION

The results and discussion can be divided into 5 sections which include 4.1) model validation, 4.2) effect of observed parameters to the cell potential in the H-SOEC, 4.3) effect of observed parameters to the hydrogen content in the H-SOEC, 4.4) regression model and 4.5) optimization

4.1 Model validation

The model validation should be performed to confirm that simulation results can predict the performance of H-SOEC. It is noted that the activation and ohmic overpotentials are considered in the electrochemical model. In this work, the concentration overpotential is omitted since its value is negligible compared with other overpotentials. The experiment of P.A. Stuart [13] is used for model validation. In their work, both electrodes of H-SOEC was made from platinum (Pt) whereas $BaCe_{0.9}Y0.1O_{3-\delta}$ (BCY10) is used as the electrolyte. The operating conditions and parameters used for model validation are listed in Table 4.1. Fig 4.1 shows the comparison results of cell potential obtained from the simulation results and the experiment data. The error of simulation result compared with the experiment is around 8%; this value is acceptable. Therefore, it can be concluded that the simulation results agree with the experimental data even though the concentration overpotential is neglect.

Table 4.1 The operating conditions and parameters used for model validation.

Active area of cell, A	0.04 m^2
Number of cell, N_{cell}	500 cell
Electrode pore radius, r	0.5 m
Electrode porosity, ξ	0.3
Electrode tortuosity [6], $\emptyset$	$(1.5\text{-}0.5\varepsilon)^{1/2}$
Electrolyte conductivity [13], $\rho_{electrolyte}$	$7.66\times10^{6}/(T\cdot\exp(-8.74\times10^{3}/T))$ $\Omega^{-1}m^{-1}$
Cell thickness of electrode, $\tau_{electrode}$	100×10^{-6} m
Cell thickness of electrolyte, $\tau_{electrolyte}$	100×10^{-6} m
Operating temperature, T	600°C, 650°C
Operating pressure, P	1 bar
Anode steam inlet composition	100% of water

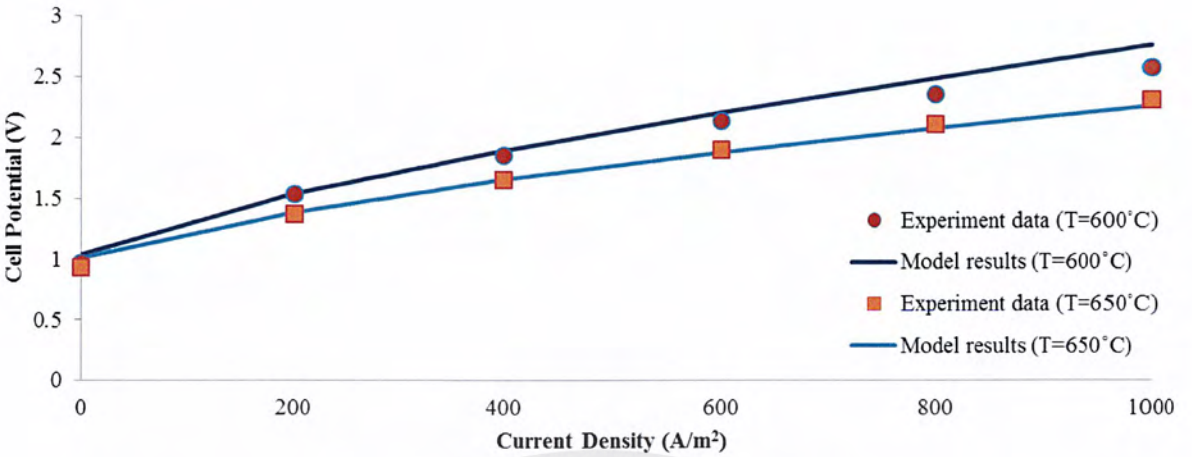

Fig. 4.1 The comparison results of the simulation results and the experiment results

4.2 Effect of operating parameters on the cell potential of the H-SOEC

4.2.1 Effect of temperature

In this section, the operating temperature is varied in a range of 450 to 800°C whereas other parameters are set as a constant value: pressure of 1 bar, current density of 250 A/m^2 and steam flow rate of 1 kmol/h. Fig. 4.2 presents the effect of operating temperature on cell potential. The simulation result indicates that the cell potential will decrease as an exponential function with increasing temperature. This is because the higher temperature operation can improve

1) Chemical reaction (electrolysis); hydrogen can occur easily.
2) Proton conductivity of electrolyte; it can reduce the ohmic overpotential

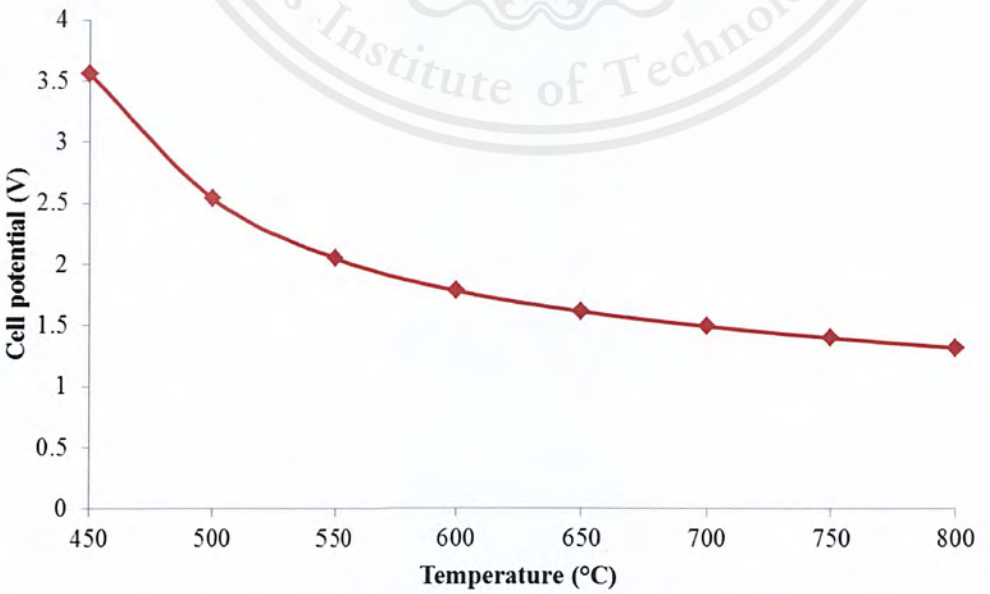

Fig. 4.2 The effect of operating temperature on cell potential at pressure of 1 bar, current density of 250 A/m^2 and steam flow rate of 100 kmol/h.

4.2.2 Effect of pressure

Fig. 4.3 demonstrates the cell potential of H-SOEC as a function of different operating pressure which is adjusted between 1 and 10 bar. The temperature, current density and steam flow rate are kept constant as 600°C , 250 A/m^2 and 1 kmol/h, respectively. In general, under higher pressure operation, the reversible potential is higher whereas the concentration overpotential is reduced. Although the concentration overpotential is neglect, an increase in reversible potential is a little value and thus, the cell potential seems no change when operating pressure increases.

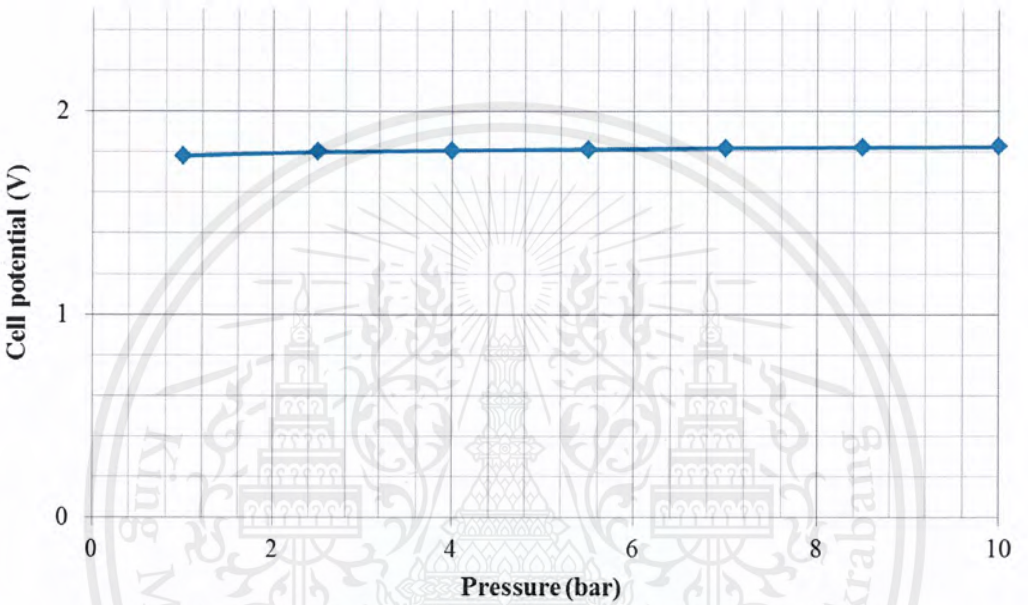

Fig. 4.3 The effect of operating pressure on cell potential at condition 600°C, 250 A/m^2 and 100 kmol/h of steam flow rate

4.2.3 Effect of current density

From the results as shown in Fig. 4.1, it can be seen that the cell potential strongly increases when H-SOEC is operated at higher current density. Increasing current density causes the important increase in overpotentials which include activation overpotentials and ohmic overpotential.

4.2.4 Important effects on the cell potential

Fig. 4.4 shows pareto chart of the standardized effects which is analyzed by Minitab software. It is found that there are two parameters: temperature and current density affected to the cell potential of H-SOEC. This can confirm the simulation results described as above. Fig. 4.5 presents the surface plot of cell potential at different temperature and current density whereas pressure and steam flow rate are set as constant value at 1 bar and 250 kmol/h, respectively. The result as

shown in Fig. 4.5 has a same trend with that in Figs. 4.2 and 4.3. The lowest cell potential can be provided when the H-SOEC is operated at high temperature and low current density.

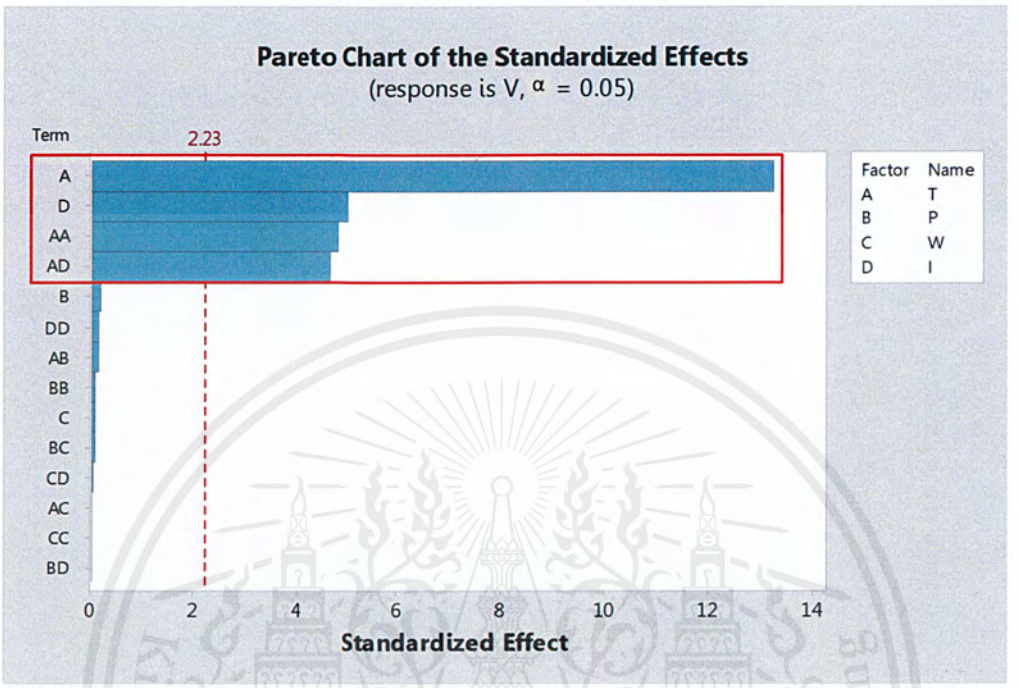

Fig. 4.4 Pareto chart of the standardized effects for cell potential responding

***Note: T=Temperature, P=Pressure, W=steam flow rate, I=Current density

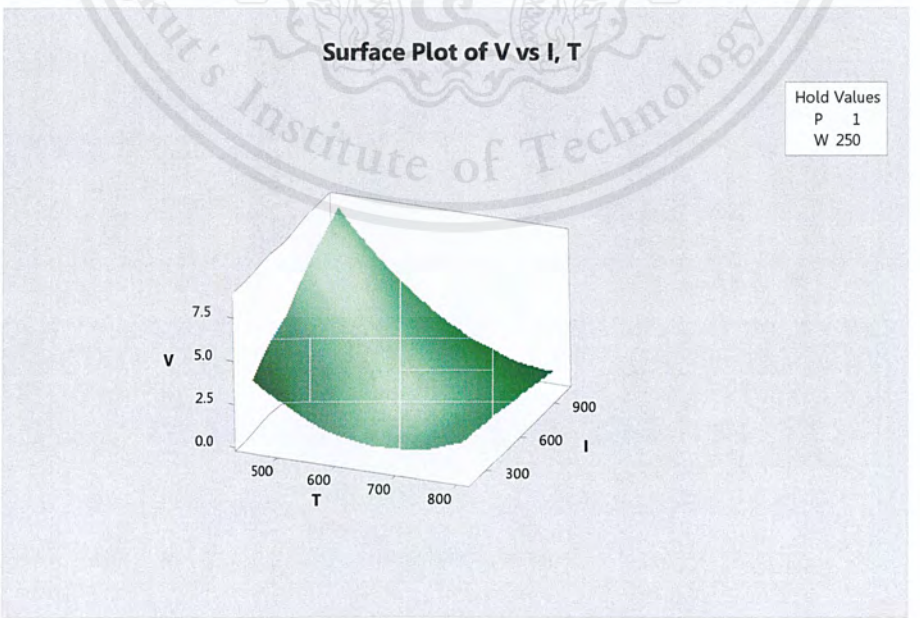

Fig. 4.5 Surface plot of the cell potential versus the current density and the temperature at pressure 1 bar and the inlet steam 250 kmol/h

4.3 Effect of operating parameters on hydrogen production from H-SOEC

4.3.1 Effect of the steam flow rate

Fig. 4.6 presents the changing of inlet steam flow rate, varied in a range of 10 to 400 kmol/h, on hydrogen production through the H-SOEC. It is noted that temperature, pressure and current density are set as a constant value at 600°C, 1 bar and 250 A/m^2, respectively. As seen in Fig. 4.6, the variation of hydrogen production can be divided into two regions. In the first region, hydrogen content strongly improves with increasing steam flow rate. It can be observed that the hydrogen content relates to inlet steam flow rate as a linear function. However, when the inlet steam flow rate is higher, the hydrogen content will constant, it can be seen in the second region that hydrogen is steadily produced. Because maximum limit of current density at 250 A/m^2 can produce 93 kmol/h of the hydrogen, according to Eq. (3.1). As a result, it can be concluded that not only steam flow rate but also current density are strongly affected on hydrogen production.

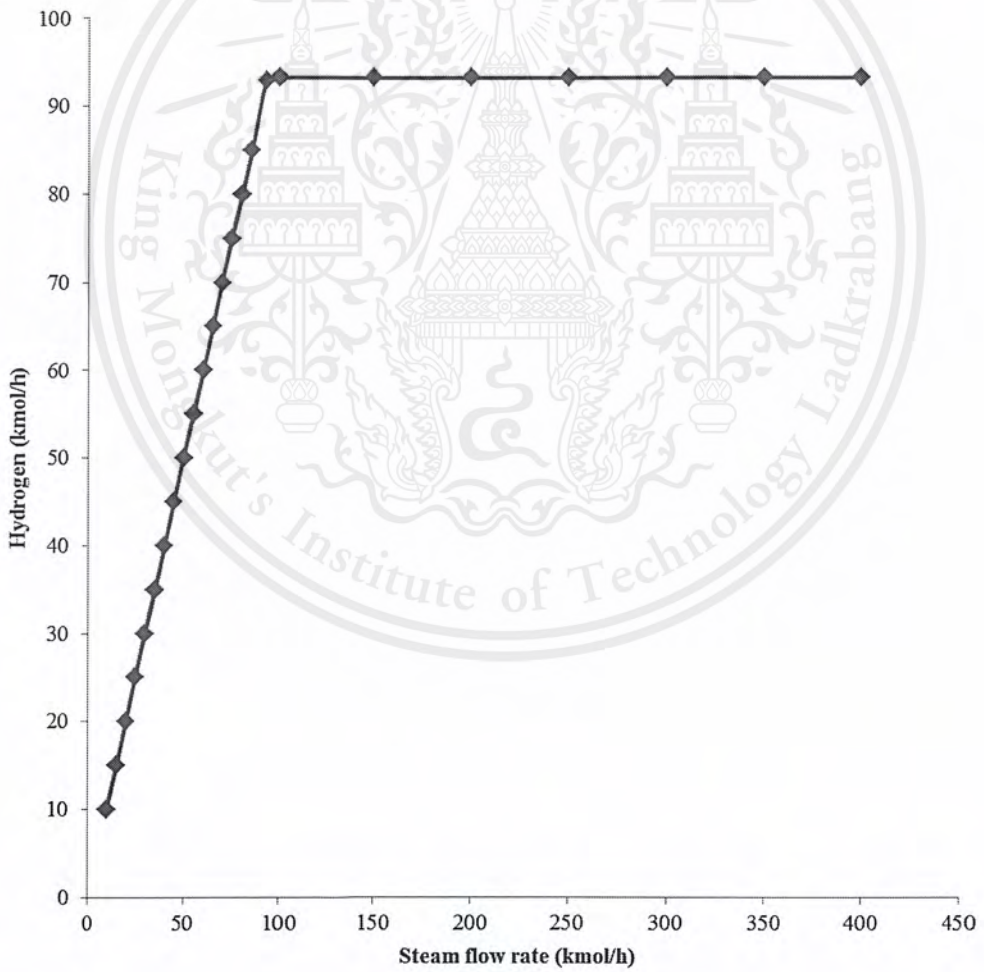

Fig. 4.6 Relation between hydrogen and steam flow rate at condition 600°C, 1 bar and 250 A/m^2

4.3.2 Effect of the current density

Fig. 4.7 shows the hydrogen production as a function of current density. In this study, the current density is varied between 200 and 1800 A/m^2 whereas other parameters are kept constant: temperature of 600°C, pressure of 1 bar and steam inlet of 400 kmol/h. It can be observed from Fig. 4.7 that hydrogen production increases as a linear function of higher current densities (200-1000 A/m^2). However, the operation at current density above 1000 A/m^2 does not affect to the hydrogen content. This is because the quantity of steam flow rate at 400 kmol/h is not enough for using in electrolysis reaction.

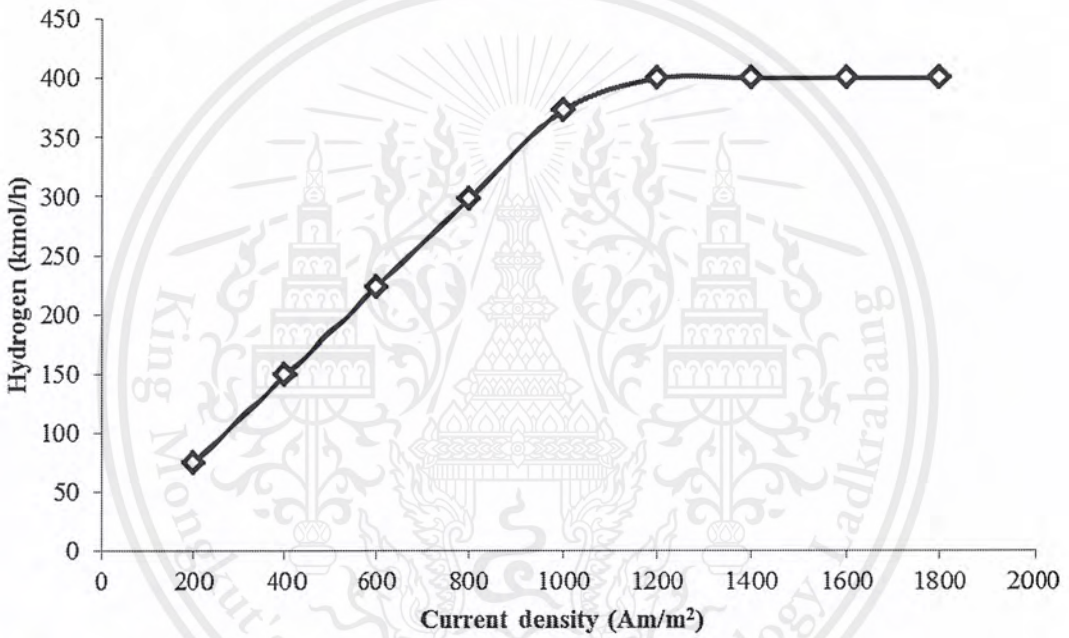

Fig. 4.7 Relation between hydrogen and current density at condition 600°C, 1 bar and 400 kmol/h of steam flow rate

4.3.3 Important effects on the hydrogen content

Pareto chart of the standardized effects on hydrogen content is demonstrated in Fig. 4.8. It is found that steam flow rate and current density are main significant effect on hydrogen production through the H-SOEC. Fig. 4.9 presents the surface plot of hydrogen content when steam flow rate and current density are varied. In this study, pressure of 1 bar and temperature are at 625°C were set as constant value. Steam flow rate and current density were

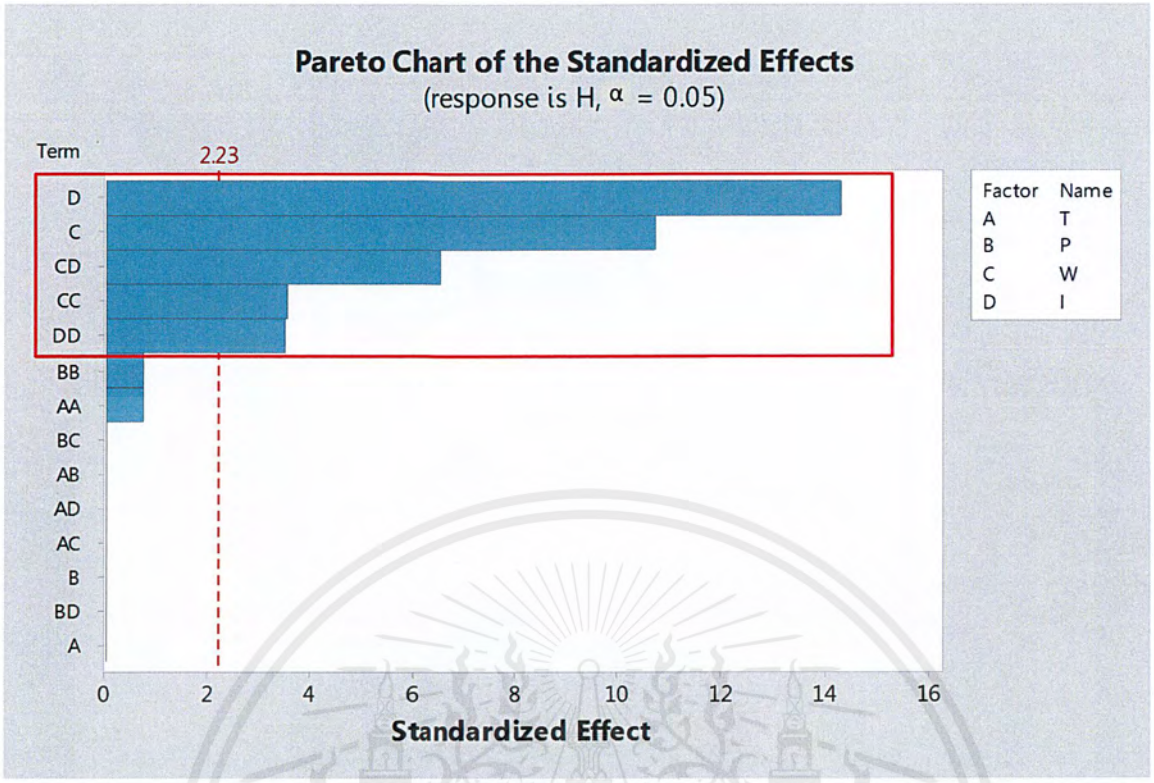

Fig. 4.8 Pareto chart of the standardized effects for hydrogen responding

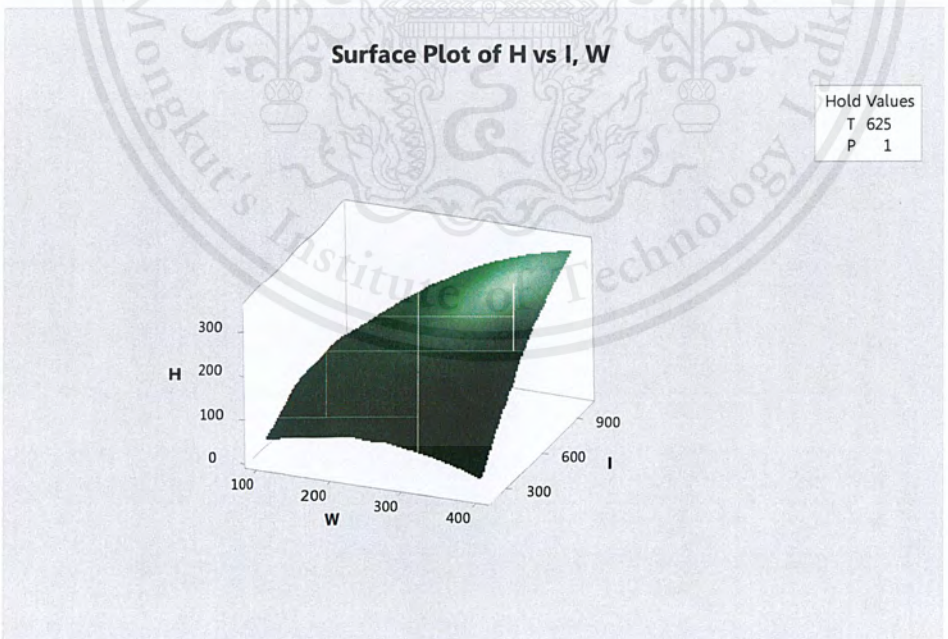

Fig. 4.9 Surface plot of the hydrogen content versus the current density and the inlet steam flow rate at temperature 625°C and pressure 1 bar

4.4 Regression model

The desire performances for H-SOEC operation are minimum cell potential (V) and maximum hydrogen content (H). These performances are affected on 4 parameters which consist of the temperature (T), the pressure (P), the steam flow rate (W) and the current density (I). The response surface method was used in optimization. The boundary of each parameter used in this study is listed as Table 4.2. The simulation results with different operating conditions designed from Box-Behnken design are shown in Table 4.3.

Table 4.2 The boundary parameters of the Box-Behnken design

Parameters	Level (-1)	Level (0)	Level (1)
T: Temperature (kmol/h)	400	625	800
P: Pressure (bar)	1	5.5	10
W: Steam flow rate (kmol/h)	100	250	400
I : Current density (A/m^2)	200	600	1000

Table 4.3 The design of the experiment and results

Run	T (°C)	P (bar)	W (kmol/h)	I (A/m^2)	H (kmol/h)	V (V)
1	450	1	250	600	223.87	6.10
2	800	1	250	600	223.87	1.54
3	450	10	250	600	223.87	6.34
4	800	10	250	600	223.87	1.60
5	625	5.5	100	200	74.62	1.63
6	625	5.5	400	200	74.62	1.56
7	625	5.5	100	1000	100.00	2.59
8	625	5.5	400	1000	373.11	2.60
9	450	5.5	250	200	74.62	3.14
10	800	5.5	250	200	74.62	1.25
11	450	5.5	250	1000	250.00	9.41
12	800	5.5	250	1000	250.00	1.76
13	625	1	100	600	100.00	2.18
14	625	10	100	600	100.00	2.13

Table 4.3 The design of the experiment and results (continue)

Run	T (°C)	P (bar)	W (kmol/h)	I (A/m^2)	H (kmol/h)	V (V)
15	625	1	400	600	223.87	2.11
16	625	10	400	600	223.87	2.15
17	450	5.5	100	600	100.00	6.33
18	800	5.5	100	600	100.00	1.58
19	450	5.5	400	600	223.87	6.31
20	800	5.5	400	600	223.87	1.55
21	625	1	250	200	74.62	1.55
22	625	10	250	200	74.62	1.60
23	625	1	250	1000	250.00	2.57
24	625	10	250	1000	250.00	2.61
25	625	5.5	250	600	223.87	2.16

The results from Table 4.4 are analyzed the variance for the regression model and the results are shown in Table 4.5. Probability value (P-value) of the parameters lower than 0.05, it has significant to the responded parameter. In the other hand, the value have no significant if P-value are higher than 0.05.

Table 4.4 The probability value analysis for regression of cell potential and hydrogen

Source	DF	Cell potential	Hydrogen
		P-Value	P-Value
Model	14	0.000	0.000
Linear	4	0.000	0.000
T	1	0.000	1.000
P	1	0.863	1.000
W	1	0.943	0.000
I	1	0.001	0.000
Square	4	0.001	0.006
T*T	1	0.001	0.473
P*P	1	0.939	0.473

Table 4.5 The probability value analysis for regression of cell potential and hydrogen (continue)

Source	DF	Cell potential	Hydrogen
		P-value	P-value
W*W	1	0.995	0.005
I*I	1	0.883	0.006
2-Way Interaction	6	0.036	0.003
T*P	1	0.885	1.000
T*W	1	0.994	1.000
T*I	1	0.001	1.000
P*W	1	0.944	1.000
P*I	1	1.000	1.000
W*I	1	0.952	0.000
Error	10		
Total	24		

*Note: DF is degree of freedom

The P-value of the cell potential, there are 4 significant parameters include;

1). T from linear model
2). I from linear model
3). T*T from square model
4). T*I from 2-way interaction

The P-value of the hydrogen, there are 5 significant parameters include;

1). W from linear model
2). I from linear model
3). W*W from square model
4). I*I from square model
5). W*I from 2-way interaction

From the above reasons, the regression models for the cell potential and the hydrogen content are reduced. The relationships of the cell potential and the hydrogen content with the significant parameters are expressed in Eqs. (4.1) and (4.2) in which R square are 96.45% and 97.50%, respectively.

$$V = 24.52 - 0.07456T + 0.01509I + 0.000059T^2 - 0.000021T * I \quad (4.1)$$

$$H = -45.8 + 0.551W + 0.1985I - 0.001613W^2 - 0.000225I^2 + 0.001138W * I \quad (4.2)$$

4.5 Optimization

The optimization can be analyzed from the results in Table 4.5 to provide minimum cell potential and maximum hydrogen content. Response optimizer in Minitab software was used to identify the combination of predictor values that jointly optimize one or more fitted responses.

The optimization plot as shown in Fig. 4.10 indicates that the temperature at 713°C and the pressure at 1 bar can provide the minimum cell potential and the maximum hydrogen content. As seen in Fig. 4.6 and 4.7, the selection of steam flow rate relates to the current density and thus, the ratio of steam flow rate (kmol/h) to current density (A/m^2) should be 1:2.681 to satisfy the Eq. (28).

From the optimization, it is found that the H-SOEC operated at the inlet steam flow rate of 372 kmol/h and current density of 1000 A/m^2 uses the cell potential as 1.49 V. Under this operation, the H-SOEC can produce 333.65 kmol/h of hydrogen. Moreover, the composite desirability is 91.75%.

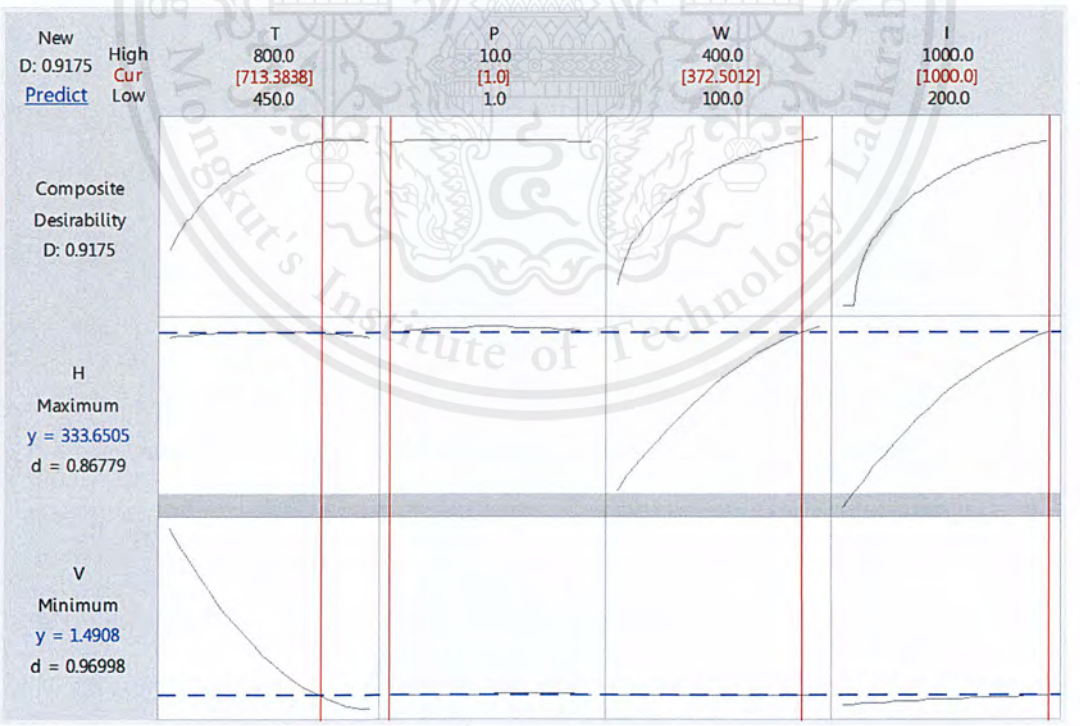

Fig. 4.10 Optimization plot for minimizing the cell potential and maximizing the hydrogen

CHAPTER V
CONCLUSIONS AND RECOMMENDATION

5.1 Conclusions

In this work, a performance of H-SOEC for hydrogen production was studied by using the Aspen plus simulator. In addition, the optimization was performed by using the Minitab software to find the optimal operating condition of H-SOEC that providing the minimum cell potential and maximum hydrogen content.

The simulation result obtained from the H-SOEC model was validated with the experiment data of P.A. Stuart [13]. It was found that the difference between the simulation result and experiment data is less than 8%. Therefore, this model can accurately predict the behavior of H-SOEC.

The effect of important parameters, i.e., temperature, steam flow rate and current density on cell potential and hygrogen content was examined. The simulation results indicated that the higher temperature and lower current density affect to ouccur the lower the cell potential whereas the higher steam flow rate and current density affect to get the higher hydrogen content.

Finally, the optimization is performed to satisfy 2 purposes which include the minimum cell potential and the maximum hydrogen content. The results revealed that the H-SOEC should be operated at 713°C under pressure of 1 bar with the inlet steam flow rate of 372 kmol/h and the current density of 1000 A/m^2. Under this operating condition, the cell potential used to produce hydrogen is 1.49 V whereas hydrogen can be produced as 333 kmol/h.

5.2 Recommendation

5.2.1 Total cost for hydrogen production of the H-SOEC should be investigated and compared with other processes for hydrogen production

5.2.2 Size of the H-SOEC should be studied and designed for optimization

REFERENCES

[1] National Aeronautics and Space Administration (NASA). Global Climate Change. https://climate.nasa.gov/vital-signs/carbon-dioxide (accessed 2017-11-15)

[2] Freedonia Group. World Hydrogen. https://www.freedoniagroup.com/industry-study/world-hydrogen-3165.htm (accessed 2017-11-15)

[3] J. Udagawa, P. Aguiar, and N. P. Brandon, "Hydrogen production through steam electrolysis: Model-based steady state performance of a cathode-supported intermediate temperature solid oxide electrolysis cell," J. Power Sources, vol. 166, no. 1, pp. 127–136, 2007.

[4] L. Bi, S. Boulfrad, and E. Traversa, "Reversible solid oxide fuel cells (R-SOFCs) with chemically stable proton-conducting oxides," Solid State Ionics, vol. 275, pp. 101–105, 2015.

[5] Fuel cell handbook, 7th ed. EG&G Technical Services, Inc., U.S. Department of Energy, Office of Fossil Energy, National Energy Technology Laboratory, P.O. Box 880, Morgantown, West Virginia, USA; November 2004. p. 57–60.

[6] Y. Xie and X. Xue, "Modeling of solid oxide electrolysis cell for syngas generation with detailed surface chemistry," Solid State Ionics, vol. 224, pp. 64–73, 2012.

[7] B.E. Poling, J.M. Prausnitz, J.P. O'connell, New York, McGraw-Hill, 2001.

[8] Y. Fu et al., "Multicomponent Gas Diffusion in Porous Electrodes," J. Electrochem. Soc., vol. 162, no. 6, pp. F613–F621, 2015.

[9] D. C. Montgomery, Design and Analysis of Experiments Eighth Edition. 1984.

[10] L. Namwong, S. Authayanun, D. Saebea, Y. Patcharavorachot, and A. Arpornwichanop, "Modeling and optimization of proton-conducting solid oxide electrolysis cell: Conversion of CO2 into value-added products," J. Power Sources, vol. 331, pp. 515–526, 2016.

[11] M. Ni, M. K. H. Leung, and D. Y. C. Leung, "Electrochemical modeling of hydrogen production by proton-conducting solid oxide steam electrolyzer," Int. J. Hydrogen Energy, vol. 33, no. 15, pp. 4040–4047, 2008.

[12] D. Grondin, J. Deseure, A. Brisse, M. Zahid, and P. Ozil, "Multiphysics Modeling and Simulation of a Solid Oxide Electrolysis Cell," pp. 42–47, 2008.

[13] P. A. Stuart, T. Unno, J. A. Kilner, and S. J. Skinner, "Solid oxide proton conducting steam electrolysers," Solid State Ionics, vol. 179, no. 21–26, pp. 1120–1124, 2008.

Appendix A
Code for Calculator Block in Aspen Plus

Constant values

```
F=96480
R=8.314
Eaa=53123
Eac=56740
kanode=2.8*(10**5)
kcathode=8.57*(10**5)
Tele=0.00045
```

Cell potential

```
V=E+NAA+NAC+NOHM
```

Ohmic overpotential

```
NOHM=j*ROHM
ROHM=Tele/Pele
Pele=7.66*10**6/T*DEXP(-8.74*10**3/T)
```

Activation overpotentials

```
NAC=R*T/F*DLOG(y+DSQRT(y**2+1))
NAA=R*T/F*DLOG(x+DSQRT(x**2+1))
X=j/(2*j0a)
Y=j/(2*j0c)
J0C=(R*T*kcathode)/(2*F)*(DEXP(-Eac/(R*T)))
J0A=(R*T*kanode)/(2*F)*(DEXP(-Eaa/(R*T)))
```

Reversible overpotentials

```
E=E0+((R*T)/(2*F))*DLOG(PH2*(PO2**0.5)/PH2O)
E0=1.253-0.00024516*T
PH2=XH2*P
PO2=XO2*P
PH2O=XH2O*P
```

Appendix B
Validation Results of the H-SOEC

Table B.1 The comparing between the experiment and the model results at 600°C

J	V		% error
	Experiment data (T=600°C)	Model results (T=600°C)	
0	0.9657	1.03893855	7.58398571
200	1.5283	1.53932582	0.721443434
400	1.8542	1.89350047	2.119537806
600	2.1311	2.19872448	3.173219464
800	2.3535	2.48168244	5.446460166
1000	2.5705	2.75280375	7.092151332

Table B.2 The comparing between the experiment and the model results at 650°C

J	V		% error
	Experiment data (T=650°C)	Model results (T=650°C)	
0	0.9322	1.00668055	7.989760781
200	1.3704	1.38185512	0.835896089
400	1.6527	1.65470107	0.121078841
600	1.8915	1.87475007	0.885536875
800	2.1031	2.07250471	1.454771052
1000	2.3037	2.25780077	1.992413509

Appendix C
Results of each parameter on the H-SOEC

Table C.1 Results of pressure effect on cell potential

P (bar)	Cell potential (V)
1	1.78164778
2.5	1.79888371
4	1.80772474
5.5	1.81371503
7	1.81825143
8.5	1.82190361
10	1.82496068

Table C.2 Results of temperature effect on cell potential

Temperature (°C)	Cell potential (V)
450	3.55733492
500	2.53674207
550	2.04979008
600	1.78164778
650	1.61208263
700	1.49079431
750	1.39527016
800	1.31506779

Table C.3 Results of steam flow rate effect on hydrogen

Steam flow rate (kmol/h)	Hydrogen (kmol/h)
10	10
15	15
20	20
25	25
30	30
35	35
40	40
45	45
50	50
55	55
60	60
65	65
70	70
75	75
80	80
85	85
100	93.278748
150	93.278748
200	93.278748
250	93.278748
300	93.278748
350	93.278748
400	93.278748

Table C.4 Results of current density effect on hydrogen

Current density ($A/m^{2)}$	Hydrogen (kmol/h)
200	74.6229984
400	149.2459968
600	223.8689952
800	298.4919936
1000	373.114992
1200	400
1400	400
1600	400
1800	400

BIBLIOGRAHPY

Name:	Mr.Chawanut Tangkusonjit
Date of Birth:	3 September 1995
Address:	172 Rd.Nakhon Sawan, Wat Sommanat, Pom Prap Sattru Phai, Bangkok 10100
E-mail:	T.Chawanut@hotmail.com
Academic Background:	Wat Bowonniwet School
Working Experience:	Internship in Yamagata University (Japan) about ZnO synthesis